2017 CMBEC40 Conference
Winnipeg MB
May 23–26, 2017

IN VITRO SIMULATION OF ELECTROPORATION USING POTATO MODEL

José Berkenbrock[1,2], Guilherme Pintarelli[2], Afrânio Antônio[2] and Daniela Suzuki[2]
[1]University of Saskatchewan, Canada. [2]Institute of Biomedical Engineering, Federal University of Santa Catarina, Brazil.

INTRODUCTION

Electrochemotherapy (ECT) and Irreversible Electroporation (IRE) for tissue ablation are two non-thermal recent techniques employed for the treatment of tumors [1], [2]. These well-established approaches exploit the physical phenomenon firstly described as a 'dielectric breakdown', but now called cell electroporation (EP, or electropermeabilization) [3]–[6]. In the cell perspective, during the application of an electric field (EF) sufficiently high to induce ~1 V transmembrane voltage, the bilayer lipid membrane experiences an electro-mechanical conformation that reduces its normal selectivity [5]. The main theory to explain this increase in conductivity considers the opening of pores around the cell poles, which are resealed after the EF is ceased [7], [8]. This is the same phenomenon behind gene electrotransfer in cell culture [9], DNA vaccines [10], or water treatment against microorganisms [11].

At the tissue level, EP is employed in food processing techniques for conservation [12], and extraction of macromolecules [13]. As aforementioned, new clinical approaches were also developed based on EP. The ECT takes advantage of the momentary pores in the cell membrane to introduce chemotherapy drugs (*e.g.* bleomycin) into tumor cells [1], [6]. That means the cells die in consequence of the drugs action. In the other hand, IRE sustain the pores opened in order to provoke cell death without additional elements [2], [14].

Over the past two decades, clinical trials have validated these therapies in humans [15], [16]. Moreover, ECT has also been successfully used for veterinary applications in several species [17]–[19]. Notwithstanding, recent works have shown the necessity of keep studying EF distribution in biological tissues. Different from homogeneous tissues, treatment application close to bones [19] and excitable tissues like heart [20] and brain [21] require attention. Numerical models are a powerful tool that has allowed scientists, engineers, physicians and veterinarians to better predict EF distribution on anatomical/physiological complex structures [2], [22], [23].

In 2004, Cima & Mir pointed the use of potato tuber as a simple, but worth experiment where the conclusions can be extended to animal tissues [24]. Potato tuber present advantages as being compatible with 3Rs concept for animal testing (Reduction of number of animals; Refinement of procedures to reduce distress; and Replacement of animal with non-animal techniques) [14], [25]. *In vivo* confirmation of ECT effectiveness may take weeks, by the tumor nodule reduction and death. Electroporated zones of potato tissue become dark around 6-12 hours after the application [14], what may enable simple and relatively fast feedback about technology effectiveness in engineering tests.

Recent studies have employed potatoes to validate the effectiveness of new electrodes sizes and configurations [26], [27], and to assess the impact of pulse parameters (*e.g.* frequency and number of pulses) [28], [29]. This work compares four numerical models, found in the literature, to *in vitro* experiments.

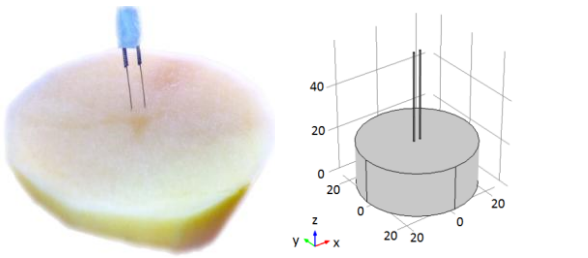

Figure 1: Needle electrodes inserted in a potato slice. (A) *in vitro* setup (B) *in silico* geometry

MATERIALS AND METHODS

In vitro preparation

Potatoes were bought at a local grocery on the day of the experiment. The EP protocol was 8 pulses with duration of 100 µs at 1 Hz [1], [22] (fig. 2). The pulse amplitudes used were 210, 270, 330 and 390 V (see table 1) between two needles 3 mm apart (fig. 1). After the procedure, the potato slices were kept in Petri dishes for 24 hours, at room temperature. Pictures were taken under constant illumination with a 10 MP, f/2.4, 30mm, autofocus, Motorola XT1058 (Schaumburg, IL, US) digital camera.

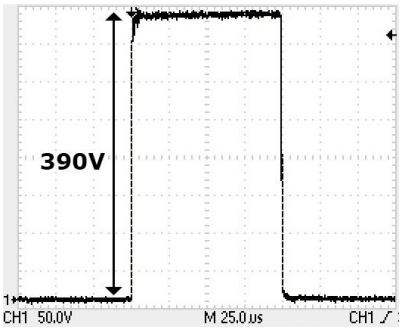

Figure 2: Applied voltage observed on oscilloscope. Data Acquisition using a Tektronix TDS 2004C (Beaverton, OR, US)

In silico design

The *in vitro* geometry was simulated by three dimensional models using COMSOL Multiphysics (COMSOL AB, Sweden). Potato slices were built with 2 cm of height, and diameter of 5 cm. The two needles had 5 cm as height, 0.6 mm as diameter and 3 mm apart. Modeled geometry is presented in the figure 1. The fine-grained mesh was automatically generated by the software, resulting 13,214 tetrahedral elements in total.

Four models were used to describe the potato tissue behavior. The first considered a constant conductivity (σ = 0.03 S/m [25]). The other three considered tissue conductivity in function of the local EF, as follows:

$$\sigma(E) = 0.03 + e^{-e^{-0.01(250-|E|)}} [S/m] \quad (1)$$

$$\sigma(E) = 0.15 + 0.6 \cdot e^{-3.153 e^{-0.00243E}} [S/m] \quad (2)$$

$$\sigma(E) = 0.03 + \frac{0.33}{1 + 10 \cdot e^{\left(\frac{65{,}000 - E}{13{,}750}\right)}} [S/m] \quad (3)$$

Equations (1)-(3) are numerical models for potato tissue conductivity that were presented by [25], [28], [29], and in this text referred as Ivorra, Neal and MIS models, respectively. Calculations were run on a personal computer (Intel Core i5-2500, 3.3 GHz, 4 GB RAM) with Windows 7 (x64, Microsoft Inc., Redmond, WA, USA) operating system. It was considered steady-state regime, and the applied EFs were 70, 90, 110 and 130 V/m, see table 1. The Dirichlet boundary condition (contact between electrodes and tissue), and Neumann (insulating external surfaces) were applied. The tissue was considered homogeneous, and the Laplace equation (4) was solved by the finite element method.

$$\nabla \cdot (\sigma \cdot \nabla V) = 0 \quad (4)$$

Where σ is the tissue conductivity [S/m], and V is the applied voltage [V].

Image processing

The image processing of *in vitro* setup was performed using MATLAB (Mathworks, USA). The detection procedure is schematized in Figure 3. Firstly the RGB image (A) is converted to gray scale (B). Hence, using a threshold rule the image is converted into black and white binary (B&W, C). Next step is to detect B&W boundaries and filter images that have a known

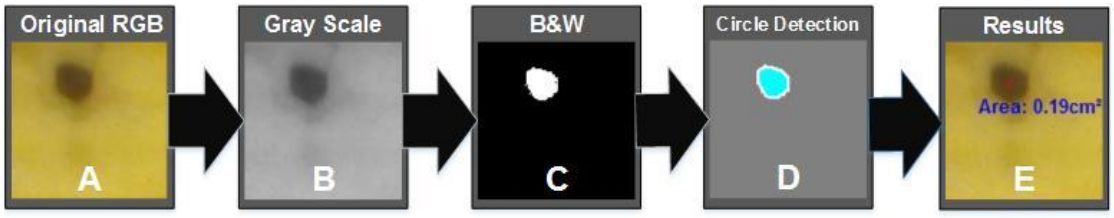

Figure 3 – Matlab image processing software diagram

Table 1: Measured browned area on potato slices 24 hours after electroporation protocol

EF [V/m]	Voltage [V]	Group I [cm²]			Group II [cm²]			Group III [cm²]			Mean
70	210	0.09	0.06	0.08	0.10	0.13	0.07	0.08	0.11	0.08	0.09
90	270	0.19	0.13	0.08	0.13	0.13	0.07	0.18	0.15	0.20	0.14
110	330	0.13	0.14	0.23	0.34	0.23	0.32	0.31	0.24	0.23	0.24
130	390	0.30	0.14	0.25	0.39	0.33	0.40	0.27	0.30	0.25	0.29

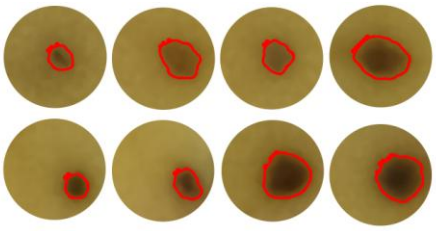

Figure 4: Browned area on potatoes

range of pixels and respect a circle tolerance. This method filter foreign objects. Finally, using a pixel to centimeters conversion, the area data is displayed in cm².

The areas from the *in silico* experiments were measured using the software ImageJ, by Color Thresholds.

RESULTS

In vitro experiments

In the figure 4 are presented 8 processed images of the 36 samples. The pictures were taken 24 hours after EP protocol, and processed using the matlab software. Control experiments showed that insertion of the needles without EFs does not produce any change.

Table 1 was filled with the values of area for all samples. In three different days (groups) the EP protocol was applied for different pulses amplitude. The mean area by applied EF is presented in the last column.

In silico experiments

In the figure 5 is presented EF distribution on potato tissue for 390 V between electrodes (130 V/m). The models were simulated in 3-D geometries, but only the top potato envelope XY-plane is shown. The figure 5.A is the model for constant conductivity (σ = 0.03 S/m), while B, C and D present results for models of Ivorra, Neal, and MIS, respectively. The color legend in the right indicates that dark red areas have the highest local EF, and dark blue means no EF.

DISCUSSION

In the last decade, potato tuber has been increasingly employed to validate new electrodes for medical devices based on EP. Such approach has been followed for both reversible and irreversible EP-based technologies [21], [26]–[29]. However, therapy approaches as ECT and IRE impose different requirements to the technology, specially about the local EF. Better understanding of EF distribution in biological tissues has been allowed through numerical models refinement allied to *in vitro* and *in vivo* studies [2], [19], [22], [23], [25], [28]. This work went through

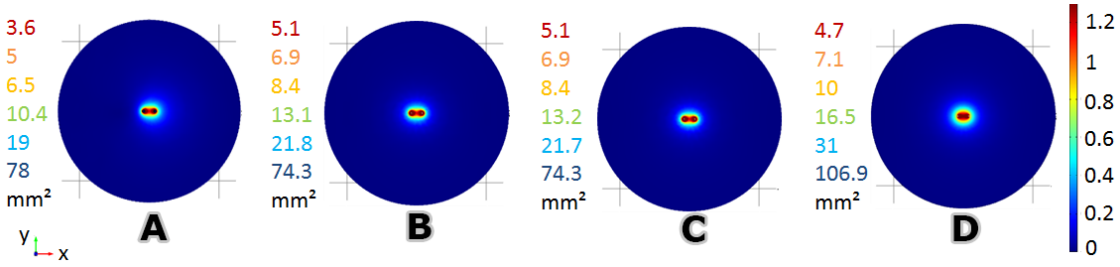

Figure 5: Simulation of electric field (EF) distribution on potato tissue for 1300 V/cm applied. The plane XY was taken from the upper slice surface. As shown by the color legend, dark red is for the highest value of local EF, while dark blue means no EF. (A) Considering constant conductivity, σ = 0.03 S/m (B) Ivorra model [25] (C) Neal model [28] and (D) MIS model [29].

four models from literature to compare *in silico* solutions to our *in vitro* results.

In the figure 4 was presented part of the *in vitro* results. The browned area was identified using a matlab code developed for this purpose. All measurements are presented in the table 1. The average values showed that browned area increased with the applied EF, which is in agreement with other studies [14], [25], [29].

Four different numerical models were simulated, and the extent of different levels of local EF were measured. In the figure 5.A is presented the result for a constant conductivity tissue, independent from the local EF. For the panels B, C and D it was considered different models that describe the tissue conductivity as function of the EF. The modification of the tissue conductivity is a dynamic process, which electroporated portions of cells modify the local EF distribution. This enable another portion of cells to electroporate, that previously could not be submitted to a high enough EF. For this reason, larger difference between models was expected to be observed. MIS model (fig. 5.D) was different from the constant model (fig. 5.A). However, the models of Ivorra and Neal were specially developed to describe the conductivity of potato tissue [25], [28], while Miklavcic's model was developed based on rabbit liver tissue, and adapted by Suárez for potato tissue [22], [29]. In the other hand, only MIS model considered the same EP protocol that was used in our *in vitro* experiments (*i.e.* 8 pulses, 100 µs, 1 Hz). This protocol is used in clinical ECT, despite some variations using 5 kHz [1]. Number of pulses, their length, frequency and amplitude are parameters that influence the EP effectiveness [5], [8]. Considering this, the difference between models seen in the figure 5 may be attributed to the number of pulses applied to the tissue [26], [29].

The browned areas from table 1 were comparable to the areas in simulation. Figure 5 presented only the data for 130 V/m, however the same methodology was applied to 70, 90 and 110 V/m [*data not presented*]. For all experiments, the *in vitro* browned areas were inside the total extent of EP *in silico*. The results of this work showed the numerical models likely predict the extent of brown areas in potato after EP protocols. In special, we could note that the *in vitro* mean of 29 mm² was closely represented *in silico* for a local electric field about 50 V/m. Ivorra *et al.* (2009) showed this value of local EF might represent irreversible EP on potato tissue, however more studies are necessary to understand the impact of pulses characteristics and variations.

CONCLUSION

The results of this work allowed to conclude that the tested numerical models may likely predict the extent of brown areas in potato after EP protocols. MIS model area of 31 mm² was in closest agreement with the 29 mm² observed *in vitro*. None of the models exactly represent our *in vitro* results, despite being based on a standardized EP protocol. Potato remain as an important subject for '*in vitro* simulations' of EP effectiveness, but more studies are necessary to determine the reversible/irreversible thresholds visually.

ACKNOWLEDGEMENTS

The authors thank the funding agencies CAPES and CNPq.

REFERENCES

[1] L. M. Mir, J. Gehl, G. Sersa, C. G. Collins, J.-R. Garbay, V. Billard, P. F. Geertsen, Z. Rudolf, G. C. O'Sullivan, and M. Marty, "Standard operating procedures of the electrochemotherapy: Instructions for the use of bleomycin or cisplatin administered either systemically or locally and electric pulses delivered by the CliniporatorTM by means of invasive or non-invasive electrodes," *Eur. J. Cancer Suppl.*, vol. 4, no. 11, pp. 14–25, Nov. 2006.

[2] R. V. Davalos, L. M. Mir, and B. Rubinsky, "Tissue Ablation with Irreversible Electroporation," *Ann. Biomed. Eng.*, vol. 33, no. 2, pp. 223–231, Feb. 2005.

[3] R. Stampfli, "Reversible electrical breakdown of the excitable membrane of a Ranvier node," *An. Acad. Bras. Ciências*, vol. 30, pp. 57–63, 1957.

[4] K. KINOSITA and T. Y. TSONG, "Formation and resealing of pores of controlled sizes in human erythrocyte membrane," *Nature*, vol. 268, no. 5619, pp. 438–441, Aug. 1977.

[5] M. R. Prausnitz, V. G. Bose, R. Langer, and J. C. Weaver, "Electroporation of mammalian skin: a mechanism to enhance transdermal drug delivery.," *Proc. Natl. Acad. Sci.*, vol. 90, no. 22, pp. 10504–10508, Nov. 1993.

[6] L. M. Mir, "Review article Therapeutic perspectives

of in vivo cell electropermeabilization q," *Bioelectrochemistry*, vol. 53, no. 1, pp. 1–10, 2000.
[7] J. Teissié and M. P. Rols, "An experimental evaluation of the critical potential difference inducing cell membrane electropermeabilization.," *Biophys. J.*, vol. 65, no. 1, pp. 409–13, Jul. 1993.
[8] D. O. H. Suzuki, A. Ramos, M. C. M. Ribeiro, L. H. Cazarolli, F. R. M. B. Silva, L. D. Leite, and J. L. B. Marques, "Theoretical and experimental analysis of electroporated membrane conductance in cell suspension," *IEEE Trans. Biomed. Eng.*, vol. 58, no. 12 PART 1, pp. 3310–3318, 2011.
[9] E. Neumann, M. Schaefer-Ridder, Y. Wang, and P. H. Hofschneider, "Gene transfer into mouse lyoma cells by electroporation in high electric fields.," *EMBO J.*, vol. 1, no. 7, pp. 841–845, 1982.
[10] S. van Drunen Littel-van den Hurk and D. Hannaman, "Electroporation for DNA immunization: clinical application," *Expert Rev. Vaccines*, vol. 9, no. 5, pp. 503–517, May 2010.
[11] S. R. Sarathy, C. Sheculski, J. Robinson, J. Walton, A. Soleymani, M. A. Kempkes, M. P. J. Gaudreau, and D. Santoro, "Design, Optimization and Scale-Up of Pulsed Electric Field Technologies for Large Flow Applications in Heterogeneous Matrices," 2016, pp. 414–417.
[12] V. Heinz, I. Alvarez, A. Angersbach, and D. Knorr, "Preservation of liquid foods by high intensity pulsed electric fields—basic concepts for process design," *Trends Food Sci. Technol.*, vol. 12, no. 3–4, pp. 103–111, Mar. 2001.
[13] T. Kotnik, W. Frey, M. Sack, S. Haberl Meglič, M. Peterka, and D. Miklavčič, "Electroporation-based applications in biotechnology," *Trends Biotechnol.*, vol. 33, no. 8, 2015.
[14] M. Hjouj and B. Rubinsky, "Magnetic Resonance Imaging Characteristics of Nonthermal Irreversible Electroporation in Vegetable Tissue," *J. Membr. Biol.*, vol. 236, no. 1, pp. 137–146, Jul. 2010.
[15] L. W. Matthiessen, H. H. Johannesen, H. W. Hendel, T. Moss, C. Kamby, and J. Gehl, "Electrochemotherapy for large cutaneous recurrence of breast cancer: A phase II clinical trial," *Acta Oncol. (Madr).*, vol. 51, no. 6, pp. 713–721, Jul. 2012.
[16] B. Mali, T. Jarm, M. Snoj, G. Sersa, and D. Miklavcic, "Antitumor effectiveness of electrochemotherapy: a systematic review and meta-analysis.," *Eur. J. Surg. Oncol.*, vol. 39, no. 1, pp. 4–16, Jan. 2013.
[17] M. Cemazar, Y. Tamzali, G. Sersa, N. Tozon, L. M. Mir, D. Miklavcic, R. Lowe, and J. Teissie, "Electrochemotherapy in Veterinary Oncology," *J. Vet. Intern. Med.*, vol. 22, no. 4, pp. 826–831, Jul. 2008.
[18] E. P. Spugnini, S. M. Renaud, S. Buglioni, F. Carocci, E. Dragonetti, R. Murace, P. Cardelli, B. Vincenzi, A. Baldi, and G. Citro, "Electrochemotherapy with cisplatin enhances local control after surgical ablation of fibrosarcoma in cats: an approach to improve the therapeutic index of highly toxic chemotherapy drugs," *J. Transl. Med.*, vol. 9, no. 1, p. 152, Dec. 2011.
[19] D. O. H. Suzuki, J. A. Berkenbrock, K. D. de Oliveira, J. O. Freytag, and M. M. M. Rangel, "Novel application for electrochemotherapy: Immersion of nasal cavity in dog," *Artif. Organs*, vol. 0, no. 1, pp. 1–11, Dec. 2016.
[20] A. Deodhar, T. Dickfeld, G. W. Single, W. C. Hamilton, R. H. Thornton, C. T. Sofocleous, M. Maybody, M. Gónen, B. Rubinsky, and S. B. Solomon, "Irreversible Electroporation Near the Heart: Ventricular Arrhythmias Can Be Prevented With ECG Synchronization," *Am. J. Roentgenol.*, vol. 196, no. 3, pp. W330–W335, Mar. 2011.
[21] M. Bonakdar, E. M. Wasson, Y. W. Lee, and R. V. Davalos, "Electroporation of Brain Endothelial Cells on Chip toward Permeabilizing the Blood-Brain Barrier," *Biophys. J.*, vol. 110, no. 2, pp. 503–513, Jan. 2016.
[22] D. Miklavcic, D. Sel, D. Cukjati, D. Batiuskaite, T. Slivnik, and L. M. Mir, "Sequential Finite Element Model of Tissue Electropermeabilisation," in *The 26th Annual International Conference of the IEEE Engineering in Medicine and Biology Society*, 2004, vol. 4, no. 5, pp. 3551–3554.
[23] A. Ramos, "Effect of the Electroporation in the Field Calculation in Biological Tissues," *Artif. Organs*, vol. 29, no. 6, pp. 510–513, Jun. 2005.
[24] L. F. Cima and L. M. Mir, "Macroscopic characterization of cell electroporation in biological tissue based on electrical measurements," *Appl. Phys. Lett.*, vol. 85, no. 19, p. 4520, 2004.
[25] A. Ivorra, L. M. Mir, and B. Rubinsky, "Electric Field Redistribution due to Conductivity Changes during Tissue Electroporation: Experiments with a Simple Vegetal Model," *IFMBE Proc.*, vol. 25, no. XIII, pp. 59–62, 2009.
[26] M. Bonakdar, E. L. Latouche, R. L. Mahajan, and R. V. Davalos, "The Feasibility of a Smart Surgical Probe for Verification of IRE Treatments Using Electrical Impedance Spectroscopy," *IEEE Trans. Biomed. Eng.*, vol. 62, no. 11, pp. 2674–2684, Nov. 2015.
[27] L. G. Campana, F. Dughiero, M. Forzan, C. R. Rossi, and E. Sieni, "A prototype of a flexible grid electrode to treat widespread superficial tumors by means of Electrochemotherapy.," *Radiol. Oncol.*, vol. 50, no. 1, pp. 49–57, Mar. 2016.
[28] R. E. Neal, P. a. Garcia, J. L. Robertson, and R. V. Davalos, "Experimental Characterization and Numerical Modeling of Tissue Electrical Conductivity during Pulsed Electric Fields for Irreversible Electroporation Treatment Planning," *IEEE Trans. Biomed. Eng.*, vol. 59, no. 4, pp. 1076–1085, Apr. 2012.
[29] C. Suárez, A. Soba, F. Maglietti, N. Olaiz, and G. Marshall, "The Role of Additional Pulses in Electropermeabilization Protocols," *PLoS One*, vol. 9, no. 12, p. e113413, 2014.